Since January 2020 Elsevier has created a COVID-19 resource centre with free information in English and Mandarin on the novel coronavirus COVID-19. The COVID-19 resource centre is hosted on Elsevier Connect, the company's public news and information website.

Elsevier hereby grants permission to make all its COVID-19-related research that is available on the COVID-19 resource centre - including this research content - immediately available in PubMed Central and other publicly funded repositories, such as the WHO COVID database with rights for unrestricted research re-use and analyses in any form or by any means with acknowledgement of the original source. These permissions are granted for free by Elsevier for as long as the COVID-19 resource centre remains active.

Immunity
Article

Structures of T Cell Immunoglobulin Mucin Receptors 1 and 2 Reveal Mechanisms for Regulation of Immune Responses by the TIM Receptor Family

César Santiago,[1] Angela Ballesteros,[1] Cecilia Tami,[2] Laura Martínez-Muñoz,[1] Gerardo G. Kaplan,[2] and José M. Casasnovas[1,*]
[1] Centro Nacional de Biotecnologia, CSIC, Campus Universidad Autónoma, 28049 Madrid, Spain
[2] Center for Biologics Evaluation and Research, Food and Drug Administration, Bethesda, MD 20892, USA
*Correspondence: jcasasnovas@cnb.uam.es
DOI 10.1016/j.immuni.2007.01.014

SUMMARY

The T cell immunoglobulin mucin (TIM) receptors are involved in the regulation of immune responses, autoimmunity, and allergy. Structures of the N-terminal ligand binding domain of the murine mTIM-1 and mTIM-2 receptors revealed an immunoglobulin (Ig) fold, with four Cys residues bridging a distinctive CC′ loop to the GFC β-sheet. The structures showed two ligand-recognition modes in the TIM family. The mTIM-1 structure identified a homophilic TIM-TIM adhesion interaction, whereas the mTIM-2 domain formed a dimer that prevented homophilic binding. Biochemical, mutational, and cell adhesion analyses confirmed the divergent ligand-binding modes revealed by the structures. Structural features characteristic of mTIM-1 appear conserved in human TIM-1, which also mediated homophilic interactions. The extracellular mucin domain enhanced binding through the Ig domain, modulating TIM receptor functions. These results explain the divergent immune functions described for the murine receptors and the role of TIM-1 as a cell adhesion receptor in renal regeneration and cancer.

INTRODUCTION

The genes coding for cellular receptors of the TIM family (also known as the Tim family) locate in an airway hyperreactivity regulatory locus linked to asthma and allergy susceptibility in mice (McIntire et al., 2001). Up to eight genes have been described in mice and three in humans (Kuchroo et al., 2003), which code for at least four cellular receptors in mice (mTIM-1, mTIM-2, mTIM-3, and mTIM-4 [also known as Tim-1, Tim-2, Tim-3, and Tim-4]) and for three receptors in humans (TIM-1, TIM-3, and TIM-4). mTIM-2 is the only murine receptor that does not have a human ortholog.

The TIM receptors are type I cell-surface glycoproteins with an N-terminal Cys-rich region followed by a mucin domain at the extracellular region, a single transmembrane region, and a cytoplasmic tail with phosphorylation motifs except in the TIM-4 receptors. Sequence identity among the N-terminal Cys-rich region of TIM homologs is about 40%, whereas between the mouse and human orthologs, it is around 60%. There are, however, marked differences in the length of the threonine-, serine-, and proline-rich mucin domain, with the number of O-linked glycosylation sites ranging from 43 in mTIM-4 to 1 in TIM-3 (Kuchroo et al., 2003).

The TIM gene family is involved in the regulation of immune responses. mTIM-1 is preferentially expressed in Th2 cells and delivers a signal that enhances T cell activation and proliferation, increasing airway inflammation and allergy (Meyers et al., 2005; Umetsu et al., 2005). In contrast, mTIM-2 is an inhibitory molecule of Th2 immune responses (Chakravarti et al., 2005; Rennert et al., 2006). mTIM-3 is mainly expressed in Th1 cells and provides a negative costimulatory signal that leads to immune tolerance (Sabatos et al., 2003; Sanchez-Fueyo et al., 2003). Polymorphisms in mTIM-1 and mTIM-3 confer susceptibility to the development of asthma and allergy (McIntire et al., 2001).

Different ligands have been described for the murine members of the TIM family. mTIM-2 binds to Semaphorin 4A and H-ferritin (Kumanogoh et al., 2002; Chen et al., 2005). mTIM-4 expressed in antigen-presenting cells binds to mTIM-1 and triggers T cell proliferation, preventing development of antigen tolerance (Meyers et al., 2005). Similar phenotype was observed by crosslinking of mTIM-1 receptor molecules with the 3B3 mAb, which activated T cells and prevented the induction of respiratory tolerance (Umetsu et al., 2005). There is less information about the functions of the human TIM receptors. The *HAVCR1* gene that codes for TIM-1 was the first member of the TIM family identified initially in monkeys and subsequently in humans as the hepatitis A virus cellular receptor 1 (HAVCR1) (Kaplan et al., 1996; Feigelstock et al., 1998b). *HAVCR1* is an important asthma determinant gene in humans (McIntire et al., 2003), and its expression is upregulated in acute kidney diseases and renal carcinoma

Table 1. Data Collection and Refinement Statistics

	Native mTIM-2	Se-Met mTIM-2	Native mTIM-1
Data Processing			
Space group	C2		$P2_12_12_1$
Cell dimensions *a*, *b*, *c* (Å)	61.5, 60.4, 69.1		44.5, 55.7, 75.5
α, β, γ (°)	90, 115.9, 90		90, 90, 90
Wavelength	0.9340	0.9330	1.0552
Resolution (Å)	25-1.5	25-2.0	25-2.5
R_{sym} or R_{merge}	7.4 (23.5)	5.0 (7.4)	8.4 (19.0)
$I/\sigma I$	6.0 (3.0)	9.9 (9.1)	7.0 (4.0)
Completeness (%)	98.6 (99.6)	100 (100)	99.8 (100)
Redundancy	3.5 (2.9)	15.9 (14.4)	5.3 (5.5)
Refinement			
Resolution (Å)	15-1.5		15-2.5
No. reflections	35890		6839
R_{work}/R_{free}	19.2/20.8		23.2/27.8
No. atoms Protein	1710		1818
Ligand/Water	4/126		4/104
B-factors Protein	17(A)/23(B)		27(A)/22(B)
Ligand/Water	11/26		49/29
Rms deviations Bond lengths (Å)	0.0052		0.0078
Bond angles (°)	1.62		1.75

Diffaction data statistics at the highest resolution shell are shown in parentheses. B factors for the molecules A and B found in the asymmetric unit of the crystals are included.

(Han and Bonventre, 2004; Vila et al., 2004). The N-terminal Cys-rich domain is critical for binding of the TIM receptors to their ligands (Thompson et al., 1998; Sabatos et al., 2003; Sanchez-Fueyo et al., 2003; Meyers et al., 2005), and the mucin domain is required for binding of mTIM-1 to mTIM-4 (Meyers et al., 2005) and for the neutralization of HAV particles by TIM-1 (Silberstein et al., 2003).

Currently, there is no structural information on the TIM receptor domains, and it is unclear how they bind to their ligands. The predicted immunoglobulin fold for the N-terminal Cys-rich domain required further verification because of the unusually high number of conserved Cys residues (six) for a single Ig domain. We pursued structure determination of the Cys-rich region for several receptors and determined the crystal structures of the N-terminal domains of mTIM-1 and mTIM-2. Our work provides a structural view on ligand-binding domains in the TIM gene family. In spite of their high sequence identity (62%), these two receptors displayed striking differences in oligomerization and presentation of ligand-binding epitopes, which explain the reported divergence in ligand recognition. The structures and derived functional data defined two distinct ligand-recognition modes in the receptor family and identified a TIM-TIM intercellular interaction in mice and humans.

RESULTS

Structure of the N-Terminal Cys-Rich Domain of TIM Receptors

We used X-ray crystallography to determine the structure of the N-terminal Cys-rich domain of TIM family members. We obtained functional domains of the mTIM-1 and mTIM-2 receptors by using bacterial expression systems and raised crystals diffracting at high resolution (Experimental Procedures). The crystal structure of the N-terminal Cys-rich region of mTIM-2 was solved first at 1.5 Å resolution, and the mTIM-1 structure was subsequently determined to a resolution of 2.5 Å (Table 1). The structures revealed an Ig domain belonging to the V set (IgV), related to the N-terminal domains of the CD4 and CAR (coxsackievirus and adenovirus receptor) cellular receptors (highest Z score in DALI search) (Holm and Sander, 1993). The IgV domains have two antiparallel β sheets with particularly short β strands B, E, and D in one face (BED β sheet) and the A, G, F, C, C′, and C″ β strands in the opposite one (GFC β sheet) (Figures 1A and 1B). A Pro residue found prior to the first Cys in all TIM receptor domains was responsible for the short length of the β strand B (Figure 1D). The first and last Cys residues in the N-terminal domain of the TIM receptors bridged the

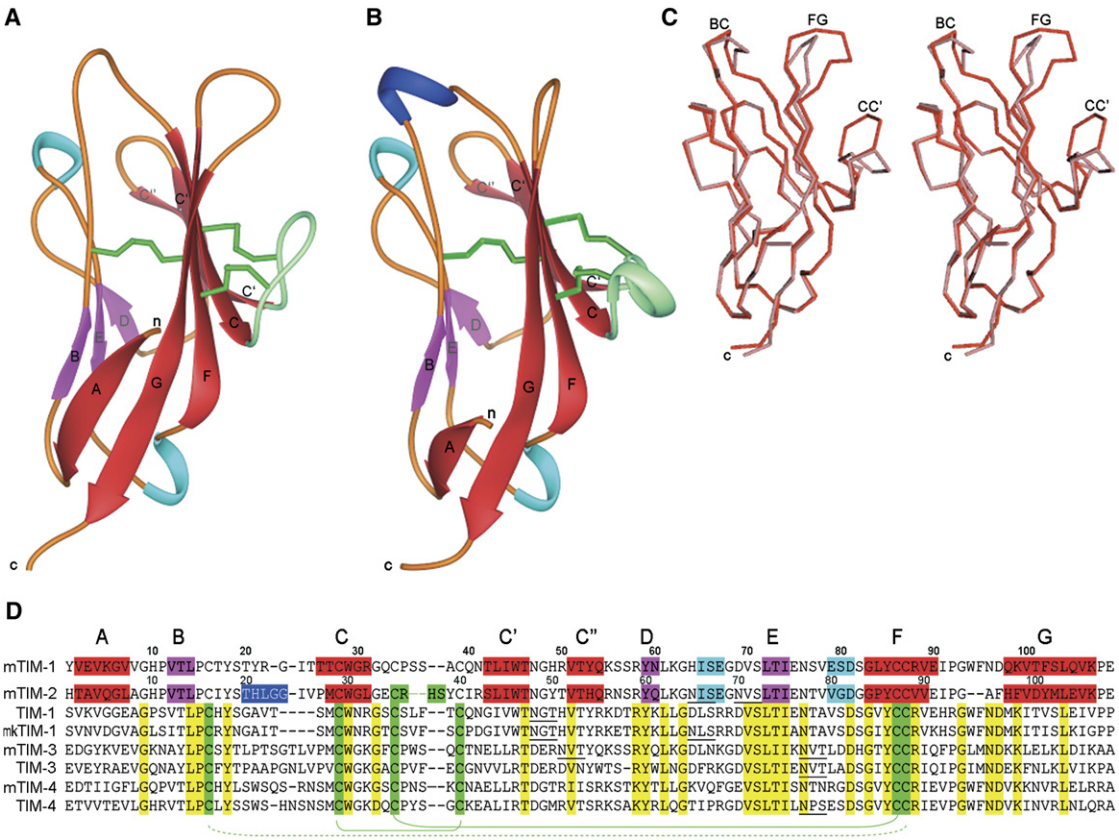

Figure 1. Crystal Structures of the N-Terminal Cys-Rich Domain of TIM Receptors

(A and B) Ribbon diagrams of the mTIM-1 and mTIM-2 structures are shown in (A) and (B), respectively. β strands of one face are red and those in the opposite side are magenta, coil is orange, 3_{10} helix is light blue, α helix in the BC loop is blue, and the loop between C and C′ β strands is light green. Cys residues and disulphide bonds are in green. Strands are labeled with uppercase letters and terminal ends (n and c) are in lowercase.

(C) Stereo view of superimposed mTIM-1 (red) and mTIM-2 (magenta) structures, with the regions showing structural variability labeled.

(D) Structural alignment of the mTIM-1 and mTIM-2 structures with residues closer than 3 Å aligned. β strands and helical regions defined by the program dssp (Wolfgang and Sander, 1983) are colored as in (A) and (B). The other TIM receptor domains were aligned by sequence. Conserved residues in most TIM receptors are colored in yellow and the six Cys residues in green. N-linked glycosylation sites are underlined and sequences of mTIM-1 and mTIM-2 numbered. Green lines join the disulphide-linked Cys residues.

β sandwich as in most Ig domains, whereas the other four Cys residues characteristic of the TIM family formed two disulphide bonds that link a long CC′ loop to the GFC β sheet (Figure 1).

The mTIM-1 and mTIM-2 N-terminal domains share 66% sequence identity and high structural similarity (Figure 1C). The rms deviation between the two structures was 0.9 Å, and the deviation between the two molecules in the asymmetric unit of the crystals was about 0.5 Å. The superimposed mTIM-1 and mTIM-2 structures showed just three misaligned regions (Figures 1C and 1D): the BC and FG loops and the interdisulphide region of the CC′ loop. The mTIM-1 BC loop was one residue shorter than the mTIM-2 loop and it did not have a helical conformation. The extended and hydrophobic mTIM-1 FG loop structure is more representative of the family than that of mTIM-2 (Figure 1D).

The mTIM-1 and mTIM-2 structures defined a common architecture for the related N-terminal domains of TIM receptors, with structural variability circumscribed to the loops at the top of the domain. The two disulphide bonds on the GFC β sheet are a distinctive structural feature of TIM IgV domains.

CC′ Loop Conformation Variability in the TIM and Related Ig Receptors

The interdisulphide region of the CC′ loop was remarkably different in the homologous mouse receptors (Figure 1C). In mTIM-2, the tip of the loop folds down and had a helical conformation, whereas in mTIM-1 it extended up onto the GFC β sheet. These differences arise from distinct contacts between residues in the loop and the β sheet (Figure 2). In mTIM-2, the aromatic ring of Tyr39 was located on the top of the helical CC′ loop and contacted the hydrophobic side chains of Val89 and Phe98, whereas the preceding residues projected toward the solvent (Figure 2A). The van der Waals interactions were not sufficient to fix the conformation of the interdisulphide region, so that

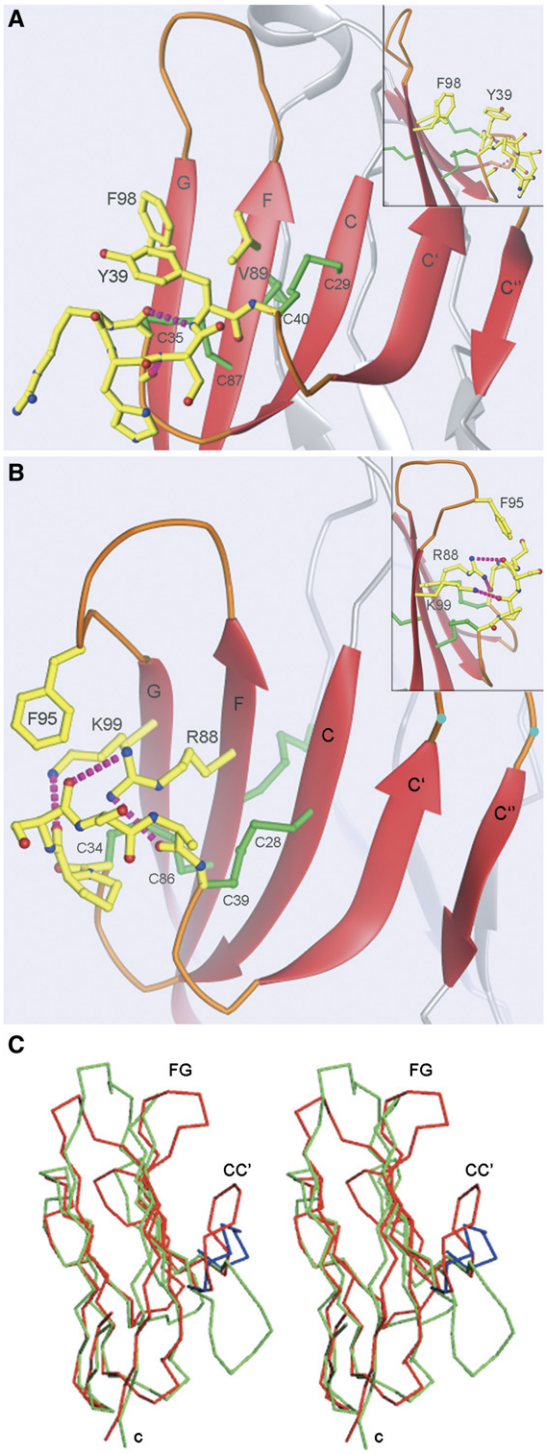

Figure 2. Conformation of the Loops Connecting C and C′ β Strands in the TIM Structures and in Related IgV Domains

(A and B) Ribbon diagram of the GFC face of the mTIM-2 (A) and mTIM-1 (B) domain structures. Insets show lateral views. Residues between the two external disulphide bonds in the CC′ loop and interacting residues at the F and G β strands and at the FG loop are yellow. Hydrogen bonds are shown as pink dashed cylinders. Oxygens and nitrogen atoms are in red and blue, respectively. Residues are labeled according to Figure 1D. Blue dots on the C′C″ loop of (B) indicate location of N-linked glycosylations in human and monkey TIM-1 and in mTIM-3.

(C) Stereo view of the superimposed mTIM-1 (red) and CAR (green, 1f5w) homologous domains. The CC′ loop region of the CEA IgV domain (1L6Z) is blue.

the tip of the solvent-exposed mTIM-2 CC′ loop remained flexible and poorly defined in the electron density maps (not shown).

In mTIM-1, the conformation of the CC′ loop tip was fixed by interactions with the Arg88 and Lys99 residues at the β strands F and G, respectively (Figure 2B). Their side chains hydrogen bonded to main-chain oxygen atoms of Pro35, Ser36, and Ala38 in the two molecules of the asymmetric unit. So, the disulphide-bridged CC′ loop was additionally linked to the upper half of the β sheet by the conserved Arg88 and Lys99 residues in the mTIM-1 structure. These basic residues are conserved in all primate and murine TIM receptors, but they are absent in mTIM-2 (Figure 1D), which has a distinct CC′ loop conformation from mTIM-1.

In addition to the described variations between the CC′ loop of mTIM-1 and mTIM-2, there were also significant differences in the conformation of the neighboring FG loop (Figure 1C). The FG loop of mTIM-1 is extended by two additional aromatic residues, Trp94 and Phe95 (Figure 1D). The side chain of Phe95 came close (~4Å) to the tip of the CC′ loop in the mTIM-1 structure (Figure 2B). Interestingly, the mTIM-1 FG loop is conserved in TIM-1 and in the human and mouse TIM-4 receptors, and the length of the loop in human TIM-3 and its mouse ortholog mTIM-3 is as in mTIM-1. The amino acid sequence similarities suggest that the conformational epitope built by the CC′ and FG loops (CC′FG epitope) on the GFC face of the mTIM-1 domain could be conserved in the TIM receptor family, except for mTIM-2 (Figure 2A). Flexibility in the long FG loop could affect the epitope conformation.

The loops connecting the C and C′ β strands are largely divergent both in length and conformation among V domains of Ig receptors (Tan et al., 2002). The CC′ loop in the TIMs was seven residues longer than in the structurally related CD4 receptor (not shown), and it had similar length but different conformation than in the homologous CAR domain (Figure 2C). In CAR the CC′ loop adopts an extended conformation, similar to other IgV domains where the GFC face is engaged in ligand recognition (Jones et al., 1992; Wang et al., 1999; van Raaij et al., 2000; Kostrewa et al., 2001), whereas in the TIM and CEA V domains, the loop folded back onto the β sheet (Figure 2C). In the CEA domain, the CC′ loop packs against an aromatic residue on the C strand (Tan et al., 2002), whereas in the TIM receptors, it is bridged by two external disulphide bonds to the GFC β sheet.

The distinctive and protruding CC′ loop onto the GFC face of the TIM IgV domains will prevent extended face-to-face intermolecular interaction through this side of the domain, observed with related Ig receptors (Jones et al., 1992; Wang et al., 1999; van Raaij et al., 2000; Kostrewa et al., 2001). Moreover, divergences on the CC′ loop conformation

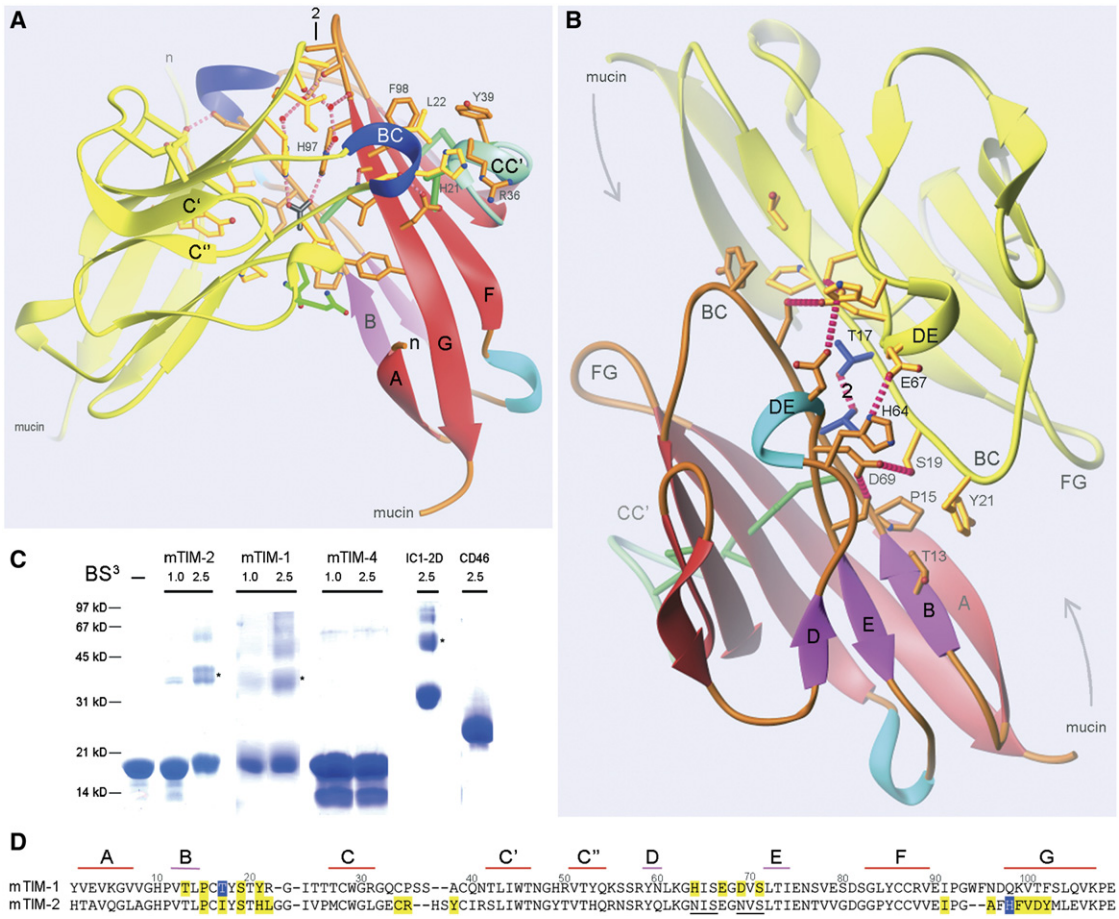

Figure 3. N-Terminal Domain Interactions in the TIM Receptors

(A and B) Ribbon diagrams of the two domains in the asymmetric unit of the mTIM-2 (A) and mTIM-1 (B) crystals. Side view of the dimer is displayed for mTIM-2, whereas a view along the quasi-2-fold axis (2) is shown for mTIM-1. Molecules presented in Figure 1 have the same coloring scheme, and the neighboring molecules are in yellow. Side chains of residues contributing to the dimer interfaces are included and some central residues are labeled. Acetate ligand found in the mTIM-2 structure is black, water molecules are red spheres, and hydrogen bonds are pink dashed cylinders. Asn residues to which glycans link in mTIM-2 are green. Arrows represent the hypothetical interaction of O-linked glycans from the C-terminal mucin domain with residues at the β strand A, BC, and FG loops of the interacting mTIM-1 domains (see also Figure S3).

(C) Self-association of the N-terminal IgV domains in solution. SDS-PAGE under reducing conditions of mTIM-1, mTIM-2, and mTIM-4 domains untreated (–) or treated with the indicated BS^3 crosslinker concentration (mM). Treated ICAM-1 protein (IC1-2D) known to dimerize at high concentration and a soluble fragment of CD46 are also included. Size and migration of the molecular weight marker is indicated. Crosslinked dimers are labeled with an asterisk. No dimerization of the mTIM-4 IgV domain is seen here or in the protein crystals (not shown).

(D) Structural alignment with residues at the dimer interface in yellow and those at the center of the interacting molecules in blue. β strands are represented by lines.

such as that of mTIM-2 could lead to differences on ligand-binding specificity among receptors of the TIM family.

A Dimeric Structure for mTIM-2

Two mTIM-2 IgV domains built up the asymmetric unit of the crystals (Figure 3A). The angle between the two mTIM-2 domains was ~60° (Figure 3A), similar to intermolecular angles reported in structures showing dimerization in *cis* of receptors linked to the same cell surface (Casasnovas et al., 1998). The buried surface area by the domain association was of 775 $Å^2$ per monomer, close to that reported for antigen-antibody complexes (800 $Å^2$) (Janin, 1997). Crosslinking experiments and analytical centrifugation revealed also self-association of the mTIM-2 IgV domains at high protein concentration in solution (Figure 3C and see Figure S1 in the Supplemental Data available online). Crosslinked dimers were observed with both mTIM-2 and mTIM-1 in conditions where dimerization was also detected for an ICAM-1 protein known to dimerize at high protein concentrations (Miller et al., 1995; Casasnovas et al., 1998). No such dimers were seen with the mTIM-4 IgV domain or a soluble CD46 receptor protein at the same protein concentration. Equilibrium sedimentation of the crystallized mTIM-2 protein (13 kDa) provided solution molecular weights of 16 and 21 kDa at low and high protein concentrations, respectively (Figure S1),

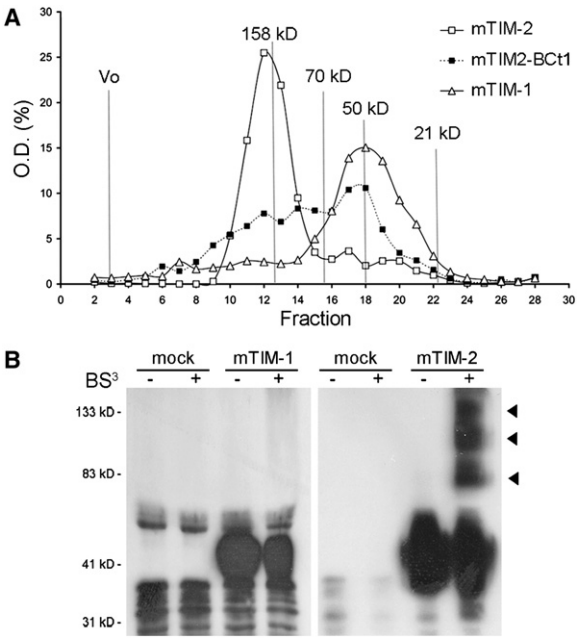

Figure 4. Oligomerization of the mTIM-2 Receptor

(A) Size exclusion chromatography of soluble mTIM-1 (open triangles) and mTIM-2 (open squares) molecules with the complete extracellular regions. mTIM2-BCt1 corresponds to a mutant mTIM-2 receptor where BC loop residues (HLG) were replaced by aligned residues in the mTIM-1 BC loop (YR). Percentage of the total optical density (OD) is plotted for each elution fraction. Exclusion volume and size of the molecular weight markers are indicated. A representative experiment is shown.

(B) Immunoblot of BS^3 treated (+) or untreated (–) cell supernatants lacking (mock) or having the indicated TIM receptor (see Experimental Procedures). The arrows mark the three mTIM-2 oligomeric species. Size and migration of the molecular weight marker are shown.

indicating IgV domain oligomerization with increasing protein concentration. The determined dimerization K_D from sedimentation was ~300 μM.

The mTIM-2 molecule dimerized through the AB edge of the IgV domain, with the helical BC loop of one molecule embracing the G strand of the neighboring domain (Figure 3A). Main intermolecular contacts included residues following the β strand B, such as the conserved Pro15, the helical BC and CC′ loops from the two interacting molecules, and residues on the FG loop and upper half of the β strand G (Figure 3D). The His97 residue that begins the β strand G was about the center of the dimer interface (labeled in Figure 3A and blue in Figure 3D). The hydrophobic cavity below the His97 side chain was occupied by an acetyl ligand, hydrogen bonded to the two neighboring histidine residues (black in Figure 3A, see Figure S2), and a network of water molecules fill up the cavity over His97 (Figure 3A). Almost 50% of the total dimerization surface was buried by the helical BC loop (365 $Å^2$) that sits on the β strand G and approached the CC′ loop of the neighboring molecule (Figure 3A). The His21 side chain on the BC loop stacked over the long Arg36 side chain in the CC′ loop, and the hydrophobic Leu22 at the tip of the BC loop inserted into a hydrophobic pocket built by Cys35, Tyr39, and Phe98 (Figure 3A). Potential N-linked glycosylation sites lay below the interdomain interface and might contribute to the stability of the mTIM-2 dimer. Therefore, IgV domain dimerization creates an extended glycan-free surface at the top of the macromolecular complex highly accessible to ligands.

Interdomain Interactions in the mTIM-1 Crystal Structure

mTIM-1 IgV domain interactions were observed in the crystals and in solution, in contrast to the homologous mTIM-4 domain (Figure 3 and Figure S1). The association of the two IgV domains in the asymmetric unit of the mTIM-1 crystals was remarkably different from mTIM-2. The mTIM-1 domains were related by a rotation angle of about 180° and had their C-terminal ends extending toward opposite directions (Figure 3B), which was suggestive of an intermolecular interaction between cell-surface receptors on opposite cell surfaces (Wang et al., 1999). The domains interact through the upper half of the BED face, including residues following the short β strand B and at the DE loop (Figures 3B and 3D). Two Thr17 residues from opposite molecules were hydrogen bonded at the center of the dimer interface. Hydrophobic contacts included Thr13 and Pro15 with the bulky Tyr21 side chain at the BC loop of a neighboring domain. Additional interacting sites between the two mTIM-1 domains engaged several residues at the long DE coil (Figures 3B and 3D). Asp69 bound to Ser19 on the BC loop of the opposite domain. Also, His64 and Glu67 were involved in interdomain interactions. Although these two residues at the helical DE loop are not conserved, some charged residues alternate at the aligned positions in the TIM receptors (Figure 1D). They could provide certain specificity for binding of TIM receptors in *trans*.

The interaction through the BED side of the mTIM-1 domains buried around 450 $Å^2$ per monomer, significantly less than that observed for the mTIM-2 IgV domains. These differences correlated with the lower dimerization constant inferred from the sedimentation experiments, where a lower solution molecular weight was determined for the mTIM-1 IgV domain at high protein concentration (Figure S1). The buried surface was also lower than the 600 $Å^2$ observed in intermolecular interactions between IgV domains of receptors binding through the GFC face (Jones et al., 1992; Wang et al., 1999; Kostrewa et al., 2001). Occupancy of a cavity between the β strand A, FG, and BC loop of the interacting domains could further stabilize the receptor interaction (Figure S3). In the crystals, the cavity was occupied by the C-terminal end of a symmetry-related domain. In the native mTIM-1 receptor, O-linked glycans from the contiguous mucin domain could penetrate in the interdomain cavity and bridge interacting receptors from opposite cells (Figure 3B). Potential glycan-interacting residues such as the basic Lys5 and Arg22, and the conserved Pro92, Trp94, and Asn96 on the FG loop lay on the upper edge of the cavity (Figure S3).

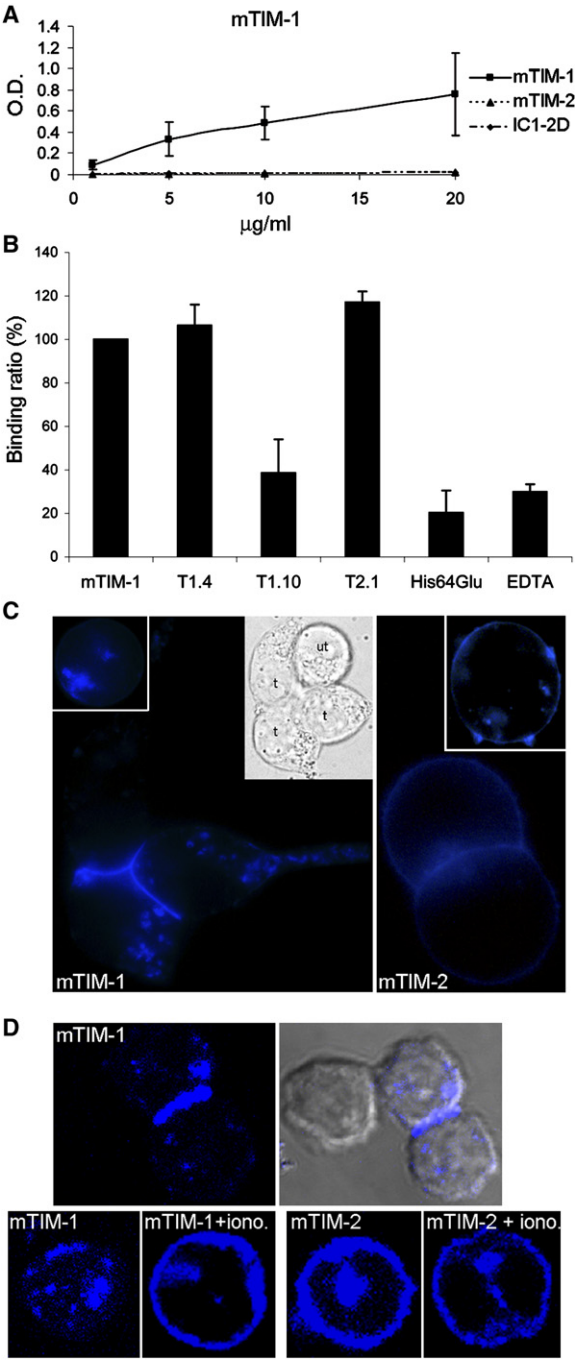

Figure 5. Homophilic mTIM-1 Receptor Interaction

(A) Binding of soluble Fc fusion proteins to plastic-coated mTIM-1 protein with the complete extracellular region. Binding to the isolated IgV domain is shown in Figure S4. TIM-Fc (mTIM-1 and mTIM-2) and control ICAM-1-Fc (IC1-2D) proteins used are included in the legend. Binding at the indicated protein concentration was determined from the optical density (OD) at 492 nm (see Experimental Procedures). Mean ± SD of three experiments is shown.

(B) Normalized binding of mTIM-1-Fc protein to plastic-coated mTIM-1 IgV in the absence (mTIM-1) or presence of mTIM-1 (T1.4 and T1.10) and mTIM-2 (T2.1) antibodies, or EDTA (10 mM). Binding of a mutant mTIM-1-Fc protein where His64 was replaced by a glutamic acid (His64Glu) is also included. Mean + SD of 6 different measurements carried with 20 and 10 μg/ml of Fc protein is shown.

(C) 293T cells transfected with the indicated TIM protein tagged with a cyan fluorescent protein (CFP) at their C-terminal ends. Fluorescence images of individual (white framed insets) and adhered cells were acquired 2 days after transfection (see Experimental Procedures). DIC image of the cell cluster with three transfected cells (t) and one cell untransfected (ut) or lacking mTIM-1 is shown in the inset.

(D) Fluorescence and DIC images of adhered 300.19 preB-cells transfected with CFP-tagged mTIM-1 are on the top. Individual transfected cells untreated or treated with 1 μg/ml of ionomycin for 30 min at 37°C are in the bottom (see also Figure S4).

Although intercellular binding of mTIM-1 to mTIM-4 has been described in the past (Meyers et al., 2005), the mTIM-1 structure provided an indication of homophilic binding in the TIM family.

mTIM-2 Receptor Oligomerization

To understand further the relevance of the mTIM-2 dimer structure and the organization of the mTIM-2 receptor on the cell surface, we analyzed oligomerization of the complete extracellular region (IgV and mucin domains) of the receptor molecule. Soluble mTIM-2 receptors secreted to cell supernatants were analyzed by size exclusion chromatography and chemical crosslinking (Figure 4). The mTIM-2 molecules eluted with an apparent molecular weight ~160 kDa (Figure 4A), whereas the size of the reduced protein was ~40 kDa (Figure 4B). In contrast, the exclusion size of the homologous mTIM-1 receptor molecule was similar to the size of the monomer. Replacement of BC loop residues (HLG, 25% of the buried surface) of mTIM-2 for the aligned residues of mTIM-1 (YR) reduced significantly (about 70%) the amount of mTIM-2 oligomer (Figure 4A), showing contribution of the BC loop to the mTIM-2 oligomerization revealed by the IgV domain structure. Oligomerization of the mTIM-2 receptors was confirmed by crosslinking experiments, where BS^3-treated samples were analyzed by SDS-PAGE (Figure 4B). Because the experiment was done under nonsaturating crosslinker concentration, most of the receptor molecules migrated as monomer (40 kDa) in the denaturing gel. Heterogeneity related to O- and N-linked glycosylation could account for the broad bands of the soluble TIM proteins. Crosslinked mTIM-2 receptor oligomers that had molecular weights around 80, 120, and 150 kDa were seen in the BS^3-treated mTIM-2 supernatants (arrows in Figure 4B). The intermediate oligomeric forms (80 and 120 kDa) could come from partial crosslinking of the high molecular weight tetrameric mTIM-2 molecule. Because the isolated N-terminal IgV domain of mTIM-2 dimerized in the crystals and in solution, it appears that the formation of the mTIM-2 receptor tetramer required the mucin domain. The absence of mTIM-1 oligomers suggested a divergence in the organization of the cellular receptors on the cell surface.

Homophilic mTIM-1 Receptor Interaction

To analyze the relevance of the TIM-TIM interaction showed by the mTIM-1 structure, we carried out both protein- and cell-binding assays (Figure 5). By using a protein-

protein binding assay, we monitored binding of soluble mTIM-1-Fc fusion proteins with the IgV and mucin domains to plastic-coated mTIM-1 proteins having either the isolated IgV domain used in crystallization (Figure S4) or the complete extracellular region of the receptor (Figure 5A). mTIM-2-Fc fusion protein did not bind to either plastic-coated mTIM-1 (Figure 5A) or mTIM-2 proteins (not shown). Homophilic mTIM-1 binding was specifically blocked by the T1.10 mAb that recognizes the IgV domain and by the addition of EDTA (Figure 5B), which indicated requirement of divalent cations for high-affinity binding and suggested involvement of carbohydrates from the mucin domain. Interestingly, the structure-guided His64Glu mutation in the DE loop of the mTIM-1 IgV domain reduced significantly the homophilic mTIM-1 binding (Figure 5B), showing a critical contribution of the DE loop and agreement with the mTIM-1 structure (Figure 3B). This mutation decreased moderately (40%) binding of mTIM-1 to mTIM-4 (not shown), suggesting binding through the BED face as well. Determined affinity for the homophilic binding in the BIAcore was about 0.6 μM (Figure S5), about 10^3 times higher than that inferred from sedimentation experiments with the isolated IgV domain. These differences showed requirement of the mucin domain and divalent cations for homophilic mTIM-1 binding, although preliminary observations indicated that the contribution of the mucin domain was more critical for mTIM-1 binding to mTIM-4 than for the homophilic interaction.

The involvement of the mTIM-1 and mTIM-2 receptors in cell-cell interactions was studied with receptor molecules that had a fluorescent protein tagged to their C-terminal intracellular domains (Figures 5C and 5D). mTIM-2 fluorescent proteins were on the surface of 293T and lymphoid cells, whereas most mTIM-1 accumulated at intracellular vesicles. However, treatment of the 300.19 lymphocytes with ionomycin or PMA enhanced localization of mTIM-1 on the cell surface (Figure 5D and Figure S4). mTIM-2 distributed quite homogenously on the surface of both isolated and interacting cells, and additive fluorescence was seen at intercellular junctions. However, mTIM-1 redistributed to the intercellular junctions of transfected cells (Figures 5C and 5D). No increase in cellular receptor was observed at the junctions of transfected and untransfected cells.

Biochemical and cellular assays presented here showed a relevant homophilic intermolecular interaction for the mTIM-1 receptor at intercellular junctions, not seen with mTIM-2. The efficient trafficking of mTIM-2 to the cell surface could be related to its oligomeric nature, whereas productive transfer of mTIM-1 to the cell surface must require rearrangements in the receptor domains induced by increasing calcium concentration.

Conservation of the mTIM-1 Structure and the Homophilic Interaction in Humans

The conformation of the CC′ and FG loops of mTIM-1 must be conserved in the human TIM-1 IgV domain. The Arg88 and Lys99 residues holding up the tip of the CC′ loop in the structure are conserved in TIM-1 (Figures 1D and 2B).

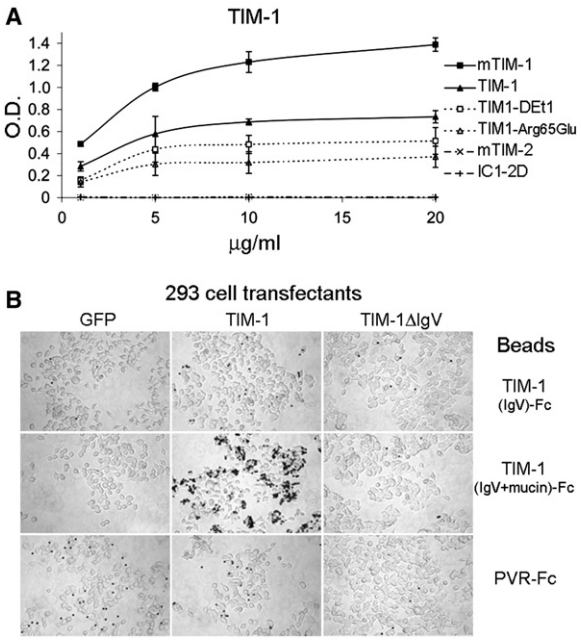

Figure 6. Homophilic TIM-1 Receptor Interaction in Humans

(A) Binding of soluble Fc fusion proteins to plastic-coated TIM-1 proteins with the complete extracellular receptor as in Figure 5A. Binding of the Arg65Glu TIM-1 mutant or a double mutant Asp62His-Arg65Glu (TIM1-DEt1) in the DE loop of the IgV domain are included.

(B) Binding of latex beads coated with the indicated protein to cells expressing GFP, the complete TIM-1 receptor, or a mutant lacking the IgV domain (TIM-1ΔIgV).

Moreover, the sequence of the FG loop is conserved also in the human and mouse TIM-1 receptors.

The presumed structural similarity between the human and mouse TIM-1 IgV domains suggested conservation of the receptors functions. Therefore, homophilic TIM-1 binding was studied both with soluble and cell-surface-expressed receptor molecules. TIM-1-Fc proteins bound to TIM-1 molecules containing the complete extracellular portion of the receptor (Figure 6A). As shown with the murine receptor, mutations in the DE loop of the TIM-1 IgV domain affected the homophilic interaction, suggesting binding through the BED face as well. Interestingly, TIM-1 bound with lower affinity than mTIM-1. This could be related to residue substitutions at the interacting surfaces, such as the Tyr21 in mTIM-1 for Ala in the human receptor (Figure 1D), which will reduce hydrophobic contacts. Beads coated with the human TIM-1-Fc protein bound specifically to TIM-1 receptors expressed on the cell surface (Figure 6B). High-affinity binding required both IgV and mucin domains, as seen with mTIM-1.

HAV Binding to TIM-1 Receptors

HAV binds specifically to the N-terminal IgV domain of the human and monkey TIM-1 receptors (Kaplan et al., 1996; Feigelstock et al., 1998b), although no binding to mTIM-1 has been detected (unpublished results). The expected structural similarity between the primate and mouse N-terminal domains allowed us to define a virus-binding

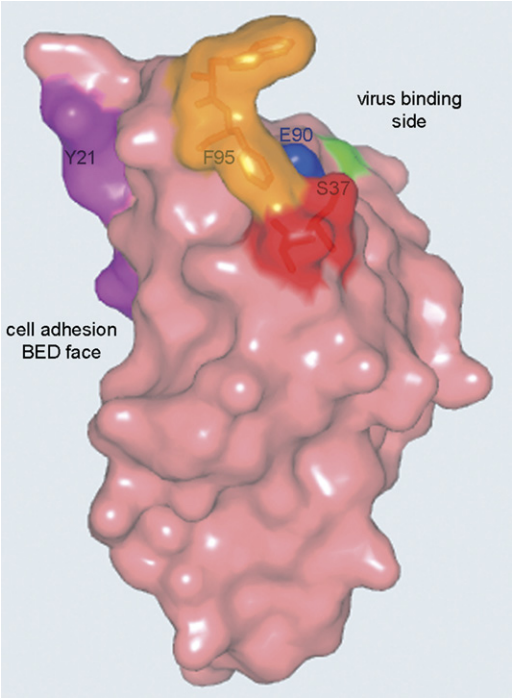

Figure 7. Ligand-Binding Surfaces in the IgV Domain of TIM-1 Receptors

Surface representation of the mTIM-1 domain structure. Surface involved in the homophilic interaction is pink. Residues in a conformational epitope built by the tip of the long CC′ loop and the FG loop onto the GFC β sheet are colored red and orange, respectively. The surface where an mkTIM-1 polymorphism (Lys88Gln) has been mapped is in blue. The mutation identified the side of the domain recognized by a mAb blocking HAV binding to its mkTIM-1 receptor (Feigelstock et al., 1998a). Surface corresponding to the Asn residue to which glycans will be linked in the primate TIM-1 receptors is green.

surface based on a gene polymorphism in monkey TIM-1 that abolished binding of a protective mAb (190/4) (Figure 7; Feigelstock et al., 1998a). This antibody blocks HAV receptor binding and protects cells from infection. The antigenic variant Lys to Gln aligns with Glu90 in mTIM-1 (blue in Figure 7), nearby the CC′FG epitope, and located the virus-binding surface on the GFC face of the IgV domain. A Glu residue is also found in human TIM-1, which binds to HAV but is not recognized by the 190/4 antibody. The protruding conformation of the CC′FG epitope and its enhanced hydrophobicity in the primate TIM-1 receptors, which have aromatic residues both in the FG and CC′ loops (Figure 1D), could be suited for HAV recognition. Moreover, the conservation of the FG loop in the primate and mouse TIM-1 IgV domains indicated that the enhanced hydrophobicity of the CC′ loop in TIM-1 could determine its virus-binding specificity (Figure 1D). The unique Phe residue in the primate receptors at the Ser37 position of the mTIM-1 CC′ loop (Figure 7) could in fact be a critical virus-binding residue, as described for a hydrophobic residue at the homologous loop in the CEA coronavirus receptor (Tan et al., 2002).

DISCUSSION

The crystal structures of the N-terminal ligand-binding domain of two TIM family members presented here have provided relevant insights for understanding the immune functions of these receptors. The structures of the related mTIM-1 and mTIM-2 showed marked differences in presentation of ligand-binding epitopes, suggestive of two distinct modes of ligand recognition. The lack of a human ortholog for mTIM-2 and the unique structural features of its IgV domain suggest an evolutionary divergence in mice and the conservation of mTIM-1-like structures in humans.

Dimerization of the N-terminal domain of mTIM-2 buries the domain surface engaged in homophilic mTIM-1 interactions, preventing mTIM-2 binding to mTIM-1 as well as homophilic mTIM-2 binding. Preliminary observations showed that disruption of the mTIM-2 dimer allowed binding to mTIM-1 (not shown). Oligomerization of the mTIM-2 receptor on the cell surface will facilitate binding to multivalent ligands (Kumanogoh et al., 2002; Chen et al., 2005). Differences on mTIM-1 and mTIM-2 organization on the cell surface could deliver distinct intracellular signals that lead to either activation or inhibition of Th2 immune responses, respectively.

The "extra" four Cys residues characteristic of the IgV domain in the TIMs fix the folded conformation of the long CC′ loop onto the GFC β sheet, defining a distinctive structural feature of the TIM family. The conformation of the loop in mTIM-2 appears to be unique within the TIM family, whereas that of mTIM-1 could be shared by other TIM receptors. Conformation of the CC′ loop in several mTIM-4 IgV domain crystal structures was almost identical to that described here for mTIM-1 (not shown). The CC′ loop appears structurally connected to the FG loop in mTIM-1, building up a protruding CC′FG epitope that partially covers the GFC β sheet. This feature suggests a divergence in ligand-recognition modes between the TIMs and related Ig receptors such as CAR, where a flat GFC face is engaged in intermolecular interactions (Jones et al., 1992; Wang et al., 1999; van Raaij et al., 2000; Kostrewa et al., 2001).

The crystal structure of mTIM-1 identified a new homophilic TIM-TIM receptor interaction in mice and humans that could be relevant for the regulation of immune functions by these receptors. Moreover, the observed trafficking of mTIM-1 to the cell surface upon lymphocyte stimulation revealed a new regulatory mechanism of TIM receptor functions. Engagement of mTIM-1 on the T cell surface by different ligands triggers a cell regulatory signal that has been linked to critical immune reactions (Meyers et al., 2005; Umetsu et al., 2005; Mesri et al., 2006). The observed clustering of mTIM-1 by homophilic binding at intercellular junctions could facilitate phosphorylation of its cytoplasmic tail, which provides a costimulatory signal for T cell activation (de Souza et al., 2005). Therefore, the homophilic mTIM-1-binding interaction described here could have important implications in the regulation of immune processes both in mice and humans and could be

responsible of the hyperproliferation of T cells observed in mice treated with soluble mTIM-1 molecules (Meyers et al., 2005). mTIM-1 is expressed on the surface of B cells and activated T cells (Meyers et al., 2005), so it is feasible that the homophilic mTIM-1 interaction mediates B-T cell adhesion interactions and has important implications in the regulation of immune responses. The conservation of the homophilic mTIM-1 receptor interaction both in mice and humans supports a conserved role in B-T cell cross-talk and its relevance in the immune system. Moreover, murine mTIM-1 and human TIM-1 receptors are overexpressed after ischemic kidney injury (Han and Bonventre, 2004), and human TIM-1 is overexpressed in renal carcinoma (Vila et al., 2004). The homophilic interaction described here suggests that TIM-1 could mediate cell adhesion interactions relevant for renal regeneration and tumor development. mTIM-1-related functions must be regulated also by receptor trafficking to the cell surface, which we show here is enhanced by increase of intracellular calcium amounts. This regulatory step could be shared by other receptors of the TIM family.

The homophilic mTIM-1 receptor binding pictured by the crystal structure revealed a striking difference with those mediated by related receptors. The IgV domains contact through their BED faces, opposite the GFC face commonly used for ligand binding by Ig receptors, which displayed a distinctive CC′FG epitope in mTIM-1. Although homophilic binding engaged the N-terminal IgV domain, experiments shown here suggested that carbohydrates from the contiguous mucin domain contribute to the interaction. O-linked glycans from the mucin domain could participate in TIM receptor interactions by occupying cavities generated upon N-terminal domain binding, such as that seen between the interacting mTIM-1 domains. Furthermore, polymorphisms in the mucin domain near the end of the IgV domain (McIntire et al., 2001) might have also some influence on the contribution of the O-linked glycans to the homophilic binding interactions, whereas those close to the membrane could modulate receptor oligomerization on the cell surface as well as intracellular receptor trafficking.

In summary, the crystal structures of the related murine mTIM-1 and mTIM-2 receptors presented here provided the structural basis for understanding ligand-binding diversity and the immune regulatory role of the TIM gene family. In contrast to the structural and functional redundancy observed in other receptor families (Wang and Springer, 1998), the structural divergence between the mTIM-1 and mTIM-2 receptors explains the marked differences in their ligand-binding specificities and functions. The lack of a human mTIM-2 ortholog suggests that mTIM-2-related functions in humans must be carried out by a cellular receptor from a related family. In contrast, sequence similarity in the mTIM-1 structural motifs between primate and murine TIM receptors suggests a conserved ligand-binding mode in the family, as well as possible homophilic TIM-TIM interactions with other TIM receptors. Conservation of the homophilic TIM-1 binding in mice and humans suggests a critical implication in the regulation of immune responses, although further investigation is now needed to determine the biological significance of this adhesion process. Moreover, structural insights coming from glycosylated TIM receptor are required for understanding the precise role of glycosylation in ligand recognition. Research extending the current knowledge on this relevant receptor family will guide the design of small molecules capable of regulating their functions in the immune system, preventing development of asthma, autoimmune diseases, and hepatitis.

EXPERIMENTAL PROCEDURES

Antibodies and cDNAs

TIM mAbs were obtained from eBioscience, Inc. The full-length cDNA coding for mTIM-1 was obtained from mouse EST #AA547594 derived from a Knowles Solter mouse 2-cell embryo cDNA library (IMAGE consortium, ATCC). The cDNA coding for full-length mTIM-2 was obtained from EST #AA509542 derived from a C57BL/6J mouse mammary gland cDNA library (IMAGE consortium, ATCC).

Protein Sample Preparation for Crystallization

Bacterial expression of the Cys-rich domains cloned into the unique NdeI and XhoI sites of the pET-27b vector (Novagen) gave insoluble inclusion bodies. However, soluble receptor domains were prepared by in vitro refolding of the inclusion bodies as described elsewhere (Jimenez et al., 2005). The mTIM-1 and mTIM-2 domains had an N-terminal Met and residues 20 to 130 and 129 of the precursor proteins, respectively (McIntire et al., 2001), a thrombin recognition site, and two protein tags included in the vector. The soluble proteins eluted from a Superdex-75 column (Amersham Biosciences) with the expected retention volume (15–20 kDa) and were recognized by the corresponding TIM monoclonal antibodies (not shown). The recombinant proteins were thrombin treated to release C-terminal tags and further purified by ion-exchange chromatography.

mTIM-1 and mTIM-2 Crystallization and Structure Determination

Crystals were initially raised with the mTIM-2 protein at 12 mg/ml by the hanging drop method and with a crystallization condition of 30% PEG-2000 methylether, 5% PEG-400, 0.2 M ammonium sulfate, 0.1 M sodium acetate (pH 4.6) and ~4% 1,2,3 heptanetriol. The mTIM-2 crystals belong to the monoclinic C2 space group, and they have two molecules in the asymmetric unit and 45% solvent content. Plate-like crystals were raised with the mTIM-1 protein domain by very similar crystallization conditions to those used for mTIM-2. The crystals belong to the orthorhombic P212121 space group and have two independent molecules in the asymmetric unit and about 37% solvent content. Details on structure determination are included in Supplemental Data; diffraction data and refinement statistics are shown in Table 1. The refined models contain all 116 amino acid residues of the mTIM-1 protein construct and all 115 amino acid residues of the crystallized mTIM-2 protein for molecule B, but the five N-terminal and the three C-terminal residues are missing for molecule A. The N-terminal residue of mTIM-1 in Figure 1D corresponds to Tyr4 in the Pdb file. The determined N-terminal His residue for the mammalian-expressed mTIM-2 receptor protein corresponds to His4 in the Pdb file.

Protein Expression in Mammalian Cells

DNAs coding for the complete extracellular region of the TIM receptors followed by a thrombin recognition site were cloned upstream of a hemagglutinin A epitope (TIM-HA) or the IgG1-Fc region (TIM-Fc) in the pEF-BOS expression vector (Jimenez et al., 2005). Serum-free cell supernatants with HA and Fc-tagged soluble receptor proteins were prepared by transient expression in 293T cells and protein concentration (10–50 μg/ml) determined by ELISA (Jimenez et al., 2005).

Mutagenesis was done by the overlapping PCR technique and confirmed by DNA sequencing. Fluorescent-tagged proteins at their cytoplasmic tails were expressed in 293T cells and in the murine 300.19 pre-B cell line by transfection with recombinant mTIM-1 and mTIM-2 cDNAs cloned in-frame with a cyan fluorescent variant of GFP (CFP) in the pECFP-N1 vector (Clontech). Cells were visualized with an Olympus IX81 confocal microscope. Confocal fluorescence and differential interference contrast (DIC) images were acquired and superimposed with the FV10-ASW 1.4 software. Fluorescent proteins were localized by excitation with a 405 nm line.

Receptor Oligomerization

Analysis of receptor oligomerization by size-exclusion chromatography was carried with TIM-HA proteins in serum-free media. Cell supernatants collected 1 day after 293T transfection with the pEF-TIM-HA construct were concentrated five times and run through a Superdex200 column with HBS buffer (20 mM HEPES and 100 mM NaCl [pH 7.5]) and 2.5 mM $CaCl_2$. The proteins in the elution fractions were detected by ELISA with HA and TIM antibodies. Molecular weight markers were run under the same conditions. Analysis of TIM-HA oligomerization by chemical crosslinking was done by BS^3 ((Bis(sulfosuccinimidyl) suberate) (Pierce) treatment of the proteins in cell supernatants collected 3 days after transfection. After overnight treatment at 4°C, the reaction was quenched with 50 mM Tris (pH 7.5), and the proteins were immunoprecipitated with anti-HA mAb (12CA5) and protein A-Sepharose and resolved by 8% SDS-PAGE under reducing conditions. Proteins were detected by immunoblot with the HA antibody and the ECL detection system (Amersham Biosciences). Chemical crosslinking of the isolated TIM IgV domains and control proteins at 5 mg/ml was carried with BS^3 for 1 hr at 4°C in HBS buffer. The samples were analyzed by 12% SDS-PAGE.

TIM-TIM Binding Assays

Binding of soluble Fc fusion proteins to plastic-coated IgV domain prepared in bacteria and TIM-1-HA proteins prepared in mammalian cells was carried in duplicate wells of 96-well plates as described elsewhere (Jimenez et al., 2005). Binding data were corrected by the background binding monitored in wells without coated proteins. A control ICAM-1-Fc (IC1-2D) protein was included in the experiments. Fc fusion proteins in cell supernatants supplemented with 5% FCS were diluted with binding buffer (20 mM Tris [pH 7.5], 100 mM NaCl, 2.5 mM $CaCl_2$, and 5% FCS). Blocking antibodies were used at 30 μg/ml.

Protein A-purified TIM-1-Fc fusion proteins were covalently coupled to 6 micron blue carboxilated microparticles as recommended by the manufacturers (Polyscience, Inc.). The poliovirus receptor (PVR) protein was included as control. 293H cells transfected with the plasmids containing cDNAs for the indicated proteins were incubated with the beads 24–48 hr after transfection in PBS with 2% FCS at room temperature. After 15–30 min, unbound beads were washed and cell monolayers in culture media examined under an inverted microscope (200×) for micrograph acquisition.

Supplemental Data

Supplemental Data include five figures and Experimental Procedures and can be found with this article online at http://www.immunity.com/cgi/content/full/26/3/299/DC1/.

ACKNOWLEDGMENTS

We acknowledge the European Synchrotron Radiation Facility for provision of synchrotron radiation facilities through the BAG-Madrid and to the BM16 beamline. We are thankful to A. Alcami for providing a BIAcore instrument, to B. Souto and G. Nurani for mTIM-2 crystallization, to C. Alfonso for ultracentrifugation experiments and to S. Prat for comments. This work was supported by grants from the Ministerio de Educacion y Ciencia of Spain (BIO2002-03281, BFU2005-05972) to J.M.C. and from the US National Institutes of Health (PO1 AI54456) and Food and Drug Administration to G.G.K. A grant from the CAM-CSIC (200520M028) to J.M.C. is also acknowledged. This paper is dedicated to the memory of J. Tormo, who started protein crystallography at CNB.

Received: November 3, 2006
Revised: January 9, 2007
Accepted: January 29, 2007
Published online: March 15, 2007

REFERENCES

Casasnovas, J.M., Stehle, T., Liu, J.-H., Wang, J.-H., and Springer, T.A. (1998). A dimeric crystal structure for the N-terminal two domains of intercellular adhesion molecule-1. Proc. Natl. Acad. Sci. USA *95*, 4134–4139.

Chakravarti, S., Sabatos, C.A., Xiao, S., Illes, Z., Cha, E.K., Sobel, R.A., Zheng, X.X., Strom, T.B., and Kuchroo, V.K. (2005). Tim-2 regulates T helper type 2 responses and autoimmunity. J. Exp. Med. *202*, 437–444.

Chen, T.T., Li, L., Chung, D.H., Allen, C.D., Torti, S.V., Torti, F.M., Cyster, J.G., Chen, C.Y., Brodsky, F.M., Niemi, E.C., et al. (2005). TIM-2 is expressed on B cells and in liver and kidney and is a receptor for H-ferritin endocytosis. J. Exp. Med. *202*, 955–965.

de Souza, A.J., Oriss, T.B., O'Malley, K.J., Ray, A., and Kane, L.P. (2005). T cell Ig and mucin 1 (TIM-1) is expressed on in vivo-activated T cells and provides a costimulatory signal for T cell activation. Proc. Natl. Acad. Sci. USA *102*, 17113–17118.

Feigelstock, D., Thompson, P., Mattoo, P., and Kaplan, G.G. (1998a). Polymorphisms of the hepatitis A virus cellular receptor 1 in African green monkey kidney cells result in antigenic variants that do not react with protective monoclonal antibody 190/4. J. Virol. *72*, 6218–6222.

Feigelstock, D., Thompson, P., Mattoo, P., Zhang, Y., and Kaplan, G.G. (1998b). The human homolog of HAVcr-1 codes for a hepatitis A virus cellular receptor. J. Virol. *72*, 6621–6628.

Han, W.K., and Bonventre, J.V. (2004). Biologic markers for the early detection of acute kidney injury. Curr. Opin. Crit. Care *10*, 476–482.

Holm, L., and Sander, C. (1993). Protein structure comparison by alignment of distance matrices. J. Mol. Biol. *233*, 123–138.

Janin, J. (1997). Specific versus non-specific contacts in protein crystals. Nat. Struct. Biol. *4*, 973–974.

Jimenez, D., Roda, P., Springer, T.A., and Casasnovas, J.M. (2005). Contribution of N-linked glycans to the conformation and function of intercellular adhesion molecules (ICAMs). J. Biol. Chem. *280*, 5854–5861.

Jones, E.Y., Davis, S.J., Williams, A.F., Harlos, K., and Stuart, D.I. (1992). Crystal structure at 2.8 Å resolution of a soluble form of the cell adhesion molecule CD2. Nature *360*, 232–239.

Kaplan, G., Totsuka, A., Thompson, P., Akatsuka, T., Moritsugu, Y., and Feinstone, S.M. (1996). Identification of a surface glycoprotein on african green monkey kidney cells as a receptor for hepatitis A virus. EMBO J. *15*, 4282–4296.

Kostrewa, D., Brockhaus, M., D'Arcy, A., Dale, G.E., Nelboeck, P., Schmid, G., Mueller, F., Bazzoni, G., Dejana, E., Bartfai, T., et al. (2001). X-ray structure of junctional adhesion molecule: structural basis for homophilic adhesion via a novel dimerization motif. EMBO J. *20*, 4391–4398.

Kuchroo, V.K., Umetsu, D.T., DeKruyff, R.H., and Freeman, G.J. (2003). The TIM gene family: emerging roles in immunity and disease. Nat. Rev. Immunol. *3*, 454–462.

Kumanogoh, A., Marukawa, S., Suzuki, K., Takegahara, N., Watanabe, C., Ch'ng, E., Ishida, I., Fujimura, H., Sakoda, S., Yoshida, K., and Kikutani, H. (2002). Class IV semaphorin Sema4A enhances T-cell activation and interacts with Tim-2. Nature *419*, 629–633.

McIntire, J.J., Umetsu, S.E., Akbari, O., Potter, M., Kuchroo, V.K., Barsh, G.S., Freeman, G.J., Umetsu, D.T., and DeKruyff, R.H. (2001).

Identification of Tapr (an airway hyperreactivity regulatory locus) and the linked Tim gene family. Nat. Immunol. *2*, 1109–1116.

McIntire, J.J., Umetsu, S.E., Macaubas, C., Hoyte, E.G., Cinnioglu, C., Cavalli-Sforza, L.L., Barsh, G.S., Hallmayer, J.F., Underhill, P.A., Risch, N.J., et al. (2003). Hepatitis A virus link to atopic disease. Nature *425*, 576.

Mesri, M., Smithson, G., Ghatpande, A., Chapoval, A., Shenoy, S., Boldog, F., Hackett, C., Pena, C.E., Burgess, C., Bendele, A., et al. (2006). Inhibition of in vitro and in vivo T cell responses by recombinant human Tim-1 extracellular domain proteins. Int. Immunol. *18*, 473–484.

Meyers, J.H., Chakravarti, S., Schlesinger, D., Illes, Z., Waldner, H., Umetsu, S.E., Kenny, J., Zheng, X.X., Umetsu, D.T., DeKruyff, R.H., et al. (2005). TIM-4 is the ligand for TIM-1, and the TIM-1-TIM-4 interaction regulates T cell proliferation. Nat. Immunol. *6*, 455–464.

Miller, J., Knorr, R., Ferrone, M., Houdei, R., Carron, C.P., and Dustin, M.L. (1995). Intercellular adhesion molecule-1 dimerization and its consequences for adhesion mediated by lymphocyte function associated-1. J. Exp. Med. *182*, 1231–1241.

Rennert, P.D., Ichimura, T., Sizing, I.D., Bailly, V., Li, Z., Rennard, R., McCoon, P., Pablo, L., Miklasz, S., Tarilonte, L., and Bonventre, J.V. (2006). T cell, Ig domain, mucin domain-2 gene-deficient mice reveal a novel mechanism for the regulation of Th2 immune responses and airway inflammation. J. Immunol. *177*, 4311–4321.

Sabatos, C.A., Chakravarti, S., Cha, E., Schubart, A., Sanchez-Fueyo, A., Zheng, X.X., Coyle, A.J., Strom, T.B., Freeman, G.J., and Kuchroo, V.K. (2003). Interaction of Tim-3 and Tim-3 ligand regulates T helper type 1 responses and induction of peripheral tolerance. Nat. Immunol. *4*, 1102–1110.

Sanchez-Fueyo, A., Tian, J., Picarella, D., Domenig, C., Zheng, X.X., Sabatos, C.A., Manlongat, N., Bender, O., Kamradt, T., Kuchroo, V.K., et al. (2003). Tim-3 inhibits T helper type 1-mediated auto- and alloimmune responses and promotes immunological tolerance. Nat. Immunol. *4*, 1093–1101.

Silberstein, E., Xing, L., van de Beek, W., Lu, J., Cheng, H., and Kaplan, G.G. (2003). Alteration of hepatitis A virus (HAV) particles by a soluble form of HAV cellular receptor 1 containing the immunoglobin-and mucin-like regions. J. Virol. *77*, 8765–8774.

Tan, K., Zelus, B.D., Meijers, R., Liu, J.-h., Bergelson, J.M., Duke, N., Zhang, R., Joachimiak, A., Holmes, K.V., and Wang, J.-h. (2002). Crystal structure of murine sCEACAM1a[1,4]:a coronavirus receptor in the CEA family. EMBO J. *21*, 2076–2086.

Thompson, P., Lu, J., and Kaplan, G.G. (1998). The Cys-rich region of hepatitis A virus cellular receptor 1 is required for binding of hepatitis A virus and protective monoclonal antidody 190/4. J. Virol. *72*, 3751–3761.

Umetsu, S.E., Lee, W.L., McIntire, J.J., Downey, L., Sanjanwala, B., Akbari, O., Berry, G.J., Nagumo, H., Freeman, G.J., Umetsu, D.T., and DeKruyff, R.H. (2005). TIM-1 induces T cell activation and inhibits the development of peripheral tolerance. Nat. Immunol. *6*, 447–454.

van Raaij, M.J., Chouin, E., van der Zandt, H., Bergelson, J.M., and Cusack, S. (2000). Dimeric structure of the coxsackievirus and adenovirus receptor D1 domain at 1.7 Å resolution. Structure *8*, 1147–1155.

Vila, M.R., Kaplan, G.G., Feigelstock, D., Nadal, M., Morote, J., Porta, R., Bellmunt, J., and Meseguer, A. (2004). Hepatitis A virus receptor blocks cell differentiation and is overexpressed in clear cell renal cell carcinoma. Kidney Int. *65*, 1761–1773.

Wang, J., and Springer, T.A. (1998). Structural specializations of immunoglobulin superfamily members for adhesion to integrins and viruses. Immunol. Rev. *163*, 197–215.

Wang, J.-h., Smolyar, A., Tan, K., Liu, J.-h., Kim, M., Sun, Z.-Y., Wagner, G., and Reinherz, E.L. (1999). Structure of a heterophilic adhesion complex between the human CD2 and CD58 (LFA-3) Counterreceptors. Cell *97*, 791–803.

Wolfgang, K., and Sander, C. (1983). Dictionary of protein secondary structure: pattern recognition of hydrogen-bonded and geometrical features. Biopolymers *22*, 2577–2637.

Accession Numbers

mTIM-1 and mTIM-2 coordinates have been deposited in the Protein Data Bank with access codes 2OR8 and 2OR7, respectively.